BACTERIAL CELLULOSE COMPOSITES FOR TARGET ANALYTE PRECONCENTRATION IN
ANALYTICAL APPLICATIONS

Mr. Panlop Lormaneenopparat

จุฬาลงกรณ์มหาวิทยาลัย
CHULALONGKORN UNIVERSITY

A Thesis Submitted in Partial Fulfillment of the Requirements
for the Degree of Master of Science in Petrochemistry and Polymer Science
Field of Study of Petrochemistry and Polymer Science
FACULTY OF SCIENCE
Chulalongkorn University
Academic Year 2020
Copyright of Chulalongkorn University

แบคทีเรียลเซลลูโลสคอมพอสิตสำหรับการเพิ่มความเข้มข้นของสารเป้าหมายในการประยุกต์ใช้ด้าน
การวิเคราะห์

นายพัลลภ หล่อมณีนพรัตน์

Thesis Title	BACTERIAL CELLULOSE COMPOSITES FOR TARGET ANALYTE PRECONCENTRATION IN ANALYTICAL APPLICATIONS
By	Mr. Panlop Lormaneenopparat
Field of Study	Petrochemistry and Polymer Science
Thesis Advisor	Professor VORAVEE HOVEN, Ph.D.
Thesis Co Advisor	NADNUDDA RODTHONGKUM, Ph.D.

Accepted by the FACULTY OF SCIENCE, Chulalongkorn University in Partial Fulfillment of the Requirement for the Master of Science

-- Dean of the FACULTY OF SCIENCE

(Professor POLKIT SANGVANICH, Ph.D.)

THESIS COMMITTEE

-- Chairman

(Professor DUANGDAO AHT-ONG, Ph.D.)

-- Thesis Advisor

(Professor VORAVEE HOVEN, Ph.D.)

-- Thesis Co-Advisor

(NADNUDDA RODTHONGKUM, Ph.D.)

-- Examiner

(Professor PATCHANITA THAMYONGKIT, Ph.D.)

-- External Examiner

(Associate Professor Atitaya Siripinyanond, Ph.D.)

พัลลภ หล่อมณีนพรัตน์ : แบคทีเรียลเซลลูโลสคอมพอสิตสำหรับการเพิ่มความเข้มข้น ของสารเป้าหมายในการประยุกต์ใช้ด้านการวิเคราะห์. (BACTERIAL CELLULOSE COMPOSITES FOR TARGET ANALYTE PRECONCENTRATION IN ANALYTICAL APPLICATIONS) อ.ที่ปรึกษาหลัก : ศ. ดร.วรวีร์ โฮเว่น, อ.ที่ปรึกษาร่วม : ดร.นาฏนัดดา รอดทองคำ

แบคทีเรียลเซลลูโลส (BC) เป็นวัสดุจากธรรมชาติที่มีสมบัติโดดเด่น ทั้งความเข้ากันได้ ทางชีวภาพ, ความสามารถในการย่อยสลายได้ตามธรรมชาติ, มีความชอบน้ำ, ความแข็งแรงเชิงกล สูง, มีรูพรุนสูง และสามารถนำมาดัดแปรสภาพทางเคมีได้หลากหลาย งานวิจัยนี้สนใจเติมคาร์บอก ซีเมทิลเซลลูโลส (CMC) ในไฮโดรเจล BC เพื่อเพิ่มความสามารถในการบวมน้ำ และป้องกันการ ยุบตัวของโครงสร้างสามมิติของแบคทีเรียลเซลลูโลสหลังผ่านการทำให้แห้ง นอกจากนี้ได้ สังเคราะห์อนุภาคนาโนทองคำ (AuNPs) ใน BC/CMC คอมพอสิตผ่านปฏิกิริยารีดักชันทางเคมี AuNPs ยังสามารถกระจายตัวได้ดีในเมทริกซ์ของ BC/CMC โดยมีขนาดเส้นผ่านศูนย์กลาง ประมาณ 13 นาโนเมตร โดย BC/CMC/AuNPs หลังผ่านการทำให้แห้งแบบแช่เยือกแข็งถูก นำไปใช้สำหรับการดูดซับสารเป้าหมาย ในการวิเคราะห์ด้วยเทคนิคเลเซอร์ดีซอร์พชันไอออไนเซ ชันแมสสเปกโทรเมทรี โดยเฉพาะอย่างยิ่ง AuNPs สามารถเป็นโพรบที่จับอย่างจำเพาะเจาะจงกับ สารที่มีไธออล เช่น กลูตาไธโอน (GSH) ซึ่งเป็นสารบ่งชี้ทางชีวภาพสำหรับโรคบางชนิด เช่น อัลไซ เมอร์ พาร์กินสัน โรคมะเร็ง โรคชรา และ โรคหัวใจ เป็นต้น โดย BC/CMC/AuNPs คอมพอสิต สามารถใช้ตรวจวัดปริมาณ GSH โดยมีความว่องไวในช่วงการตรวจวัด 50 – 10,000 นาโนโมลาร์ และมีขีดจำกัดในการตรวจวัดที่ต่ำ ประมาณ 54.1 นาโนโมลาร์ ซึ่งมีความเป็นไปได้ในการคัดแยก ระหว่างคนปกติและผู้ป่วยอัลไซเมอร์

สาขาวิชา   ปิโตรเคมีและวิทยาศาสตร์พอลิ   ลายมือชื่อนิสิต ....
เมอร์
ปีการศึกษา   2563   ลายมือชื่อ อ.ที่ปรึกษาหลัก ....
ลายมือชื่อ อ.ที่ปรึกษาร่วม ....

6172018023 : MAJOR PETROCHEMISTRY AND POLYMER SCIENCE

KEYWORD: bacterial cellulose, carboxymethyl cellulose, gold nanoparticles, thiol-containing biomarker, ldi-ms

Panlop Lormaneenopparat : BACTERIAL CELLULOSE COMPOSITES FOR TARGET ANALYTE PRECONCENTRATION IN ANALYTICAL APPLICATIONS. Advisor: Prof. VORAVEE HOVEN, Ph.D. Co-advisor: NADNUDDA RODTHONGKUM, Ph.D.

Bacterial cellulose (BC) is a well-known natural material with desirable properties including biocompatibility, biodegradability, hydrophilicity, high mechanical strength, high porosity, and broad chemically modifiable capacity. Herein, we incorporate carboxymethyl cellulose (CMC) in BC hydrogel to improve the swelling property and prevent collapsing of 3D bacterial cellulose network upon drying. In addition, gold nanoparticles (AuNPs) were successfully embedded within the BC/CMC composite using *in situ* chemical reduction. Moreover, AuNPs were uniformly distributed in BC/CMC matrix with a diameter of approximately 13 nm. The freeze-dried BC/CMC/AuNPs composite was subsequently used for adsorption of targeted analytes for laser desorption/ionization mass spectrometry. In particular, AuNPs can act as the selective capture probes for thiol-containing compounds, such as glutathione (GSH) that is an important biomarker of some diseases, such as Alzheimer's, Parkinson's, cancer, aging and heart problem. BC/CMC/AuNPs composite showed the high sensitivity towards GSH detection with a linear range of 50 – 10,000 nM and a limit of detection as low as 54.1 nM, which is promising for distinguishing between normal and Alzheimer's patients.

Field of Study:	Petrochemistry and Polymer Science	Student's Signature ....
Academic Year:	2020	Advisor's Signature ....
		Co-advisor's Signature ....

ACKNOWLEDGEMENTS

TABLE OF CONTENTS

LIST OF FIGURES

จุฬาลงกรณ์มหาวิทยาลัย

CHULALONGKORN UNIVERSITY

LIST OF TABLES

จุฬาลงกรณ์มหาวิทยาลัย
CHULALONGKORN UNIVERSITY

LIST OF ABBREVIATION

AgNPs	Silver nanoparticles
ATR-FTIR	Attenuated total reflection Fourier-transform infrared spectroscopy
AuNPs	Gold nanoparticle
BC	Bacterial cellulose
CMC	Carboxymethyl cellulose
DLS	Dynamic Light Scattering
DS	Degree of substitution
DTG	Derivative Thermogravimetry
FE-SEM	Field emission scanning electron microscopy
GCE	Glassy carbon electrode
GOx	Glucose oxidase
GSH	Glutathione
ICP-AES	Inductively coupled plasma atomic emission spectroscopy
JIS	Japanese industrial standard
Lac	Laccase
LDI-MS	laser desorption/ionization mass spectrometry
LOD	Limit of detection
MCEM	Mixed cellulose ester membrane
MTX	Methotrexate
PAA	Poly(acrylic acid)
PDI	Polydispersity index
RAFT	Reversible addition–fragmentation chain transfer
SALDI-MS	Surface-assisted laser desorption/ionization mass spectrometry
TEM	Transmission electron microscopy
TGA	Thermogravimetric analysis
UV-Vis	UV-visible spectroscopy
XRD	X-ray Diffraction

CHAPTER I

INTRODUCTION

1.1   Introduction

Bacterial cellulose (BC) is a polysaccharide-based material that can be generated extracellularly by bacteria.[1] Its unique characteristics include a three dimensional (3D) porous network structure having high-purity cellulose nanofibers, high crystallinity, and good mechanical property. The as-synthesized BC exhibits excellent hydrogel-like swelling property that makes it suitable for many applications such as food industry[2], textile[3] and medicine[4]. Due to strong hydrogen bonding among BC nanofibers, BC network would collapse upon drying and lose the ability to rehydrate.[5] To overcome the problem, carboxymethyl cellulose (CMC) which is a negatively charged polyelectrolyte was used to incorporate into the BC matrix. [6] The resulting BC/CMC hydrogel shows a satisfactory reswelling property after drying. With such favorable characteristics, it is anticipated that the same material can also be used for other analytical applications in which high water absorption capacity is demanded for aqueous-based analyte collection and also perhaps preconcentration. Moreover, BC can be incorporated with nanomaterials[7] for specific applications such as silver nanoparticle (AgNPs)[8, 9]. and gold nanoparticle (AuNPs)[10, 11] that can be used for analytical applications.
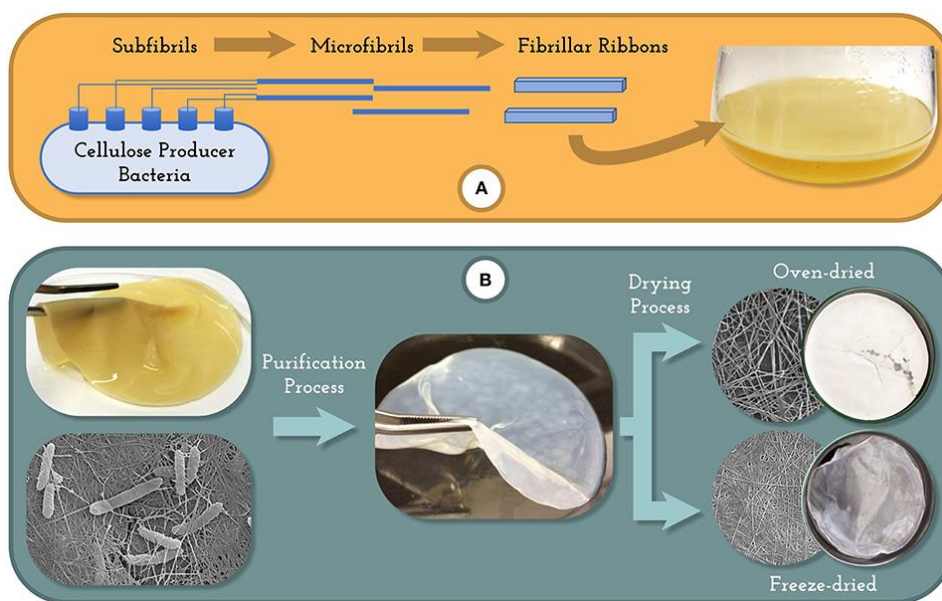
Figure 1.1 Biosynthesis (A) and downstream processing (B) of bacterial cellulose.[2]

In 2020, de Lima Fontes, et.al[12] developed BC/CMC biocomposites using different degree of substitution (DS) of CMC from 0.7 to 1.2. The BC/CMC was prepared by *in situ* modification of a static culture medium using *Gluconacetobacter xylinus* bacteria. The result showed that the BC/CMC composite prepared from CMC with DS of 0.7 exhibited the highest liquid uptake around 958%. The biocomposite were loaded with methotrexate (MTX) which is a poorly water soluble drug used for the topical treatment of psoriasis. The MTX-loaded hydrogel showed a typical burst release effect in the first 15 min. However, the BC/CMC with DS of 0.9 promoted a slight lowering of MTX release rate.
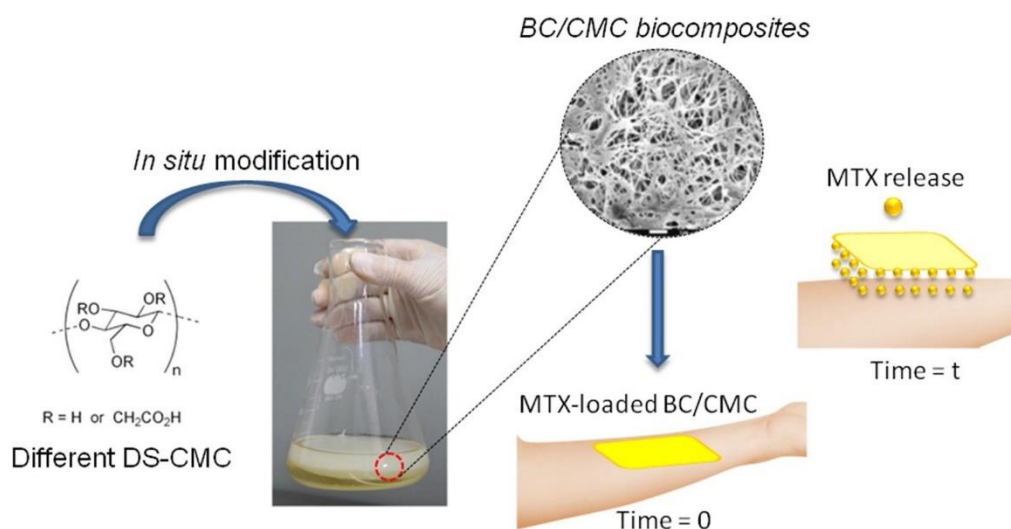
Figure 1.2 Schematic illustration of the BC/CMC biocomposites preparation for topical release of MTX.[12]

In 2021, Siripongpreda and coworkers[13] prepared BC/CMC hydrogel by direct deposition of negatively charged polyelectrolyte, CMC into BC matrix. The BC membrane was directly immersed in CMC solution which is a simple and low-cost method without special tool requirement. The CMC diffuses in between BC fibers that make the BC hydrogel reswellable after air-drying. The water absorption capacity of the BC/CMC hydrogel as a function of the soaking time and CMC concentration. The BC/CMC hydrogel was used as the non-invasive colorimetric sensor for sweat pH and glucose. The fabricated BC/CMC based pH sensor exhibited a fast response over a pH range of 4.0 – 9.0 by naked eye observation. Meanwhile, the fabricated BC/CMC based glucose sensor was based on the color development of KI by hydrogen peroxide from enzymatic reaction of glucose oxidase (GOx) which exhibited a low limit of detection (LOD) of 25 µM and a wide linear detection range 0.0-0.5 mM by portable spectrometer. The developed BC/CMC hydrogel is a potential platform for non-invasive sensors for sweat pH and glucose on-skin health monitoring.
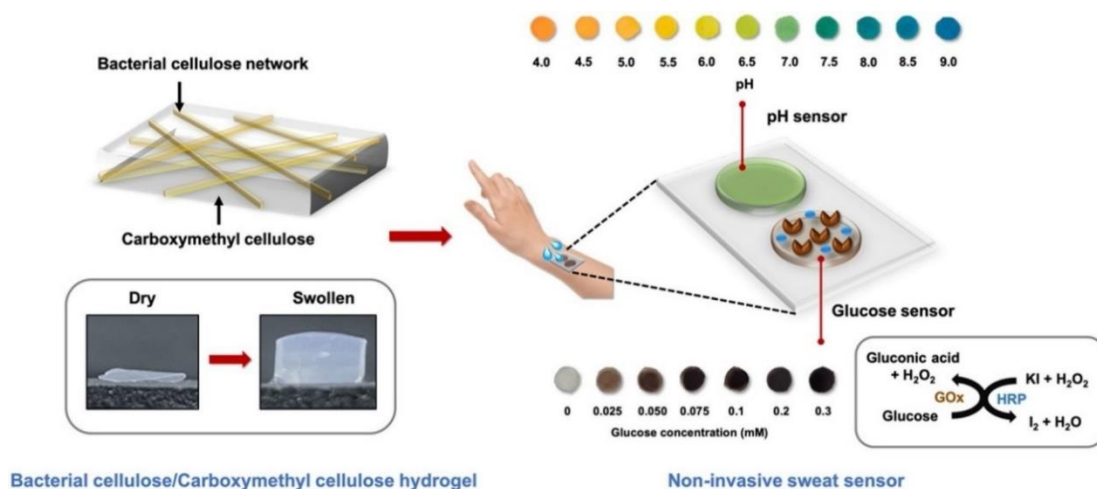
Figure 1.3 Schematic representation of BC/CMC-based re-swellable hydrogel as colorimetric sensor of sweat pH and glucose.[13]

In 2015, Li and coworkers[14] prepared BC-AuNPs hybrid nanofibers via electrostatic-assembly *in situ* chemical reduction methods. AuNPs were successfully deposited on the surface of BC nanofibers. Then, the BC-AuNPs hybrid nanofibers were attached onto the glassy carbon electrode (GCE) surface. A certain amount of laccase (lac) and Nafion were also deposited on the GCE to be used as working electrode for biosensing. The electrochemical biosensor was performed to detect hydroquinone which is an environmental pollutant. The developed biosensor can detect hydroquinone in lake water with LOD as low as 5.71 nM and a linear range of 30 – 100 nM.
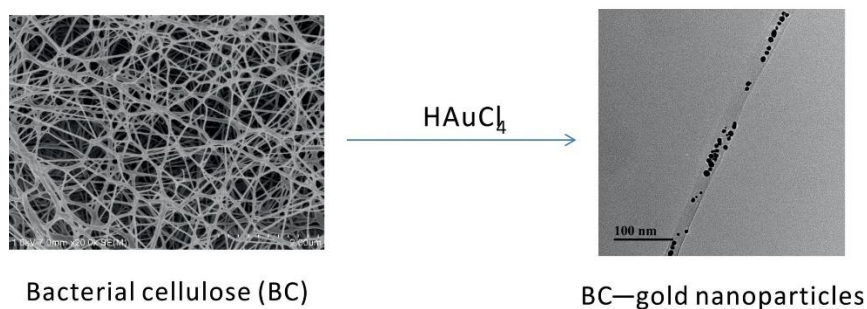
Figure 1.4 The BC-AuNPs hybrid nanofiber by in situ chemical reduction.[13]

In 2015, Morales-Narváez and coworkers[15] developed various BC nanopapers as optical sensing platforms which contained nanomaterial including of AgNPs, AuNPs, CdSe@ZnS quantum dots and $NaYF_4$:Yb^{3+}@Er^{3+}&SiO_2 up-conversion nanoparticles. The AgNPs/BC and AuNPs-BC were synthesized by using hydroxyl groups of BC as reducing moieties for chemical reduction of Ag^+ and Au^{3+}, respectively. The obtained AgNPs/BC was used as plasmonic nanopapers for colorimetric detection by monitoring UV–vis absorption spectra after absorption of methimazole and iodine. Meanwhile, the AuNPs-BC was used for sensing thiourea and cyanide by a similar concept. Moreover, BC was modified by carboxylation to generate carboxyl group (COOH). The carboxylated BC was therefore conjugated with CdSe@ZnS quantum dots and $NaYF_4$:Yb^{3+}@Er^{3+}&SiO_2 up-conversion nanoparticles to produce photoluminescent sensing platform.
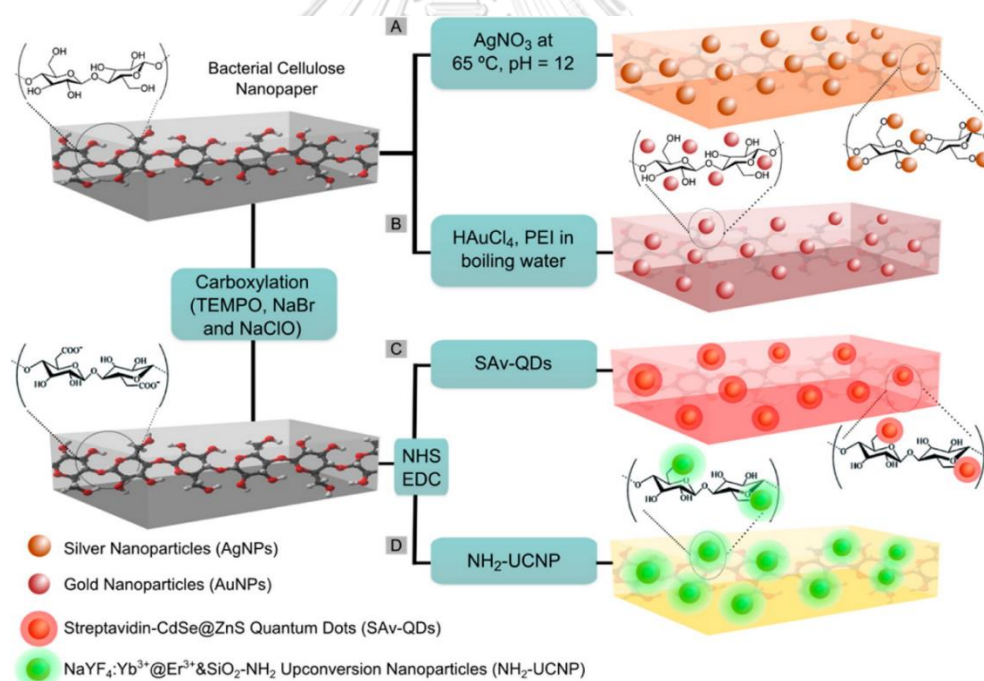
Figure 1.5 Schematic of the nanopaper-based composites. (A and B) fabrication of plasmonic nanopaper: (A) AgNPs/BC nanopaper; (B) AuNPs/BC nanopaper . (C and D) fabrication of photoluminescent nanopaper: (C) CdSe@ZnS quantum dot/BC; (D) $NaYF_4$:Yb^{3+}@Er^{3+} up-conversion nanoparticle/BC.[15]

Biomarkers are biological compound that are measurable in biological media such as human tissue, cell, or fluids. Biomarkers have been used as indicator for medical diagnosis or treatment of disease.[16] For example, glutathione (GSH) is a thiol-containing peptide which is an important biomarker in human. GSH is an antioxidant and a tripeptide composed of l-cysteine, glycine, and γ-glutamic acid, that can prevent damage to important cellular components caused by reactive oxygen species such as free radicals and peroxides.[17] GSH level can be used as a diagnostic biomarker of some diseases, such as Alzheimer's, Parkinson's, cancer, aging and heart problem.[18] In Alzheimer's patient, GSH level in plasma become decreased to 84% as compared with normal.[19] Analysis of biomarker generally requires sensitive analytical method such as electrochemistry[20], fluorescence spectroscopy[21]. UV-visible spectroscopy[22], surface plasmon resonance[23] and mass spectrometry.[24] Laser desorption/ionization mass spectrometry (LDI-MS) is a widely used technique for biomarker identification due to its high sensitivity and accuracy.[25] AuNPs, in particular, are suitable nanomaterials with high selectivity towards thiol-containing compounds so that they can be used as selective probes of thiol-containing biomarker for LDI-MS analysis. AuNPs absorb laser energy and transfer to analyte in the ionization step that is appropriate for samples with low mass range (300 – 1300 m/z).[26]

In 2013, Li et. al.[27] developed AuNPs-modified mixed cellulose ester membrane (AuNPs-MCEM) and used as substrate for LDI-MS analysis. The AuNPs-MCEM was used for determination of iodide (I⁻) ions when I⁻ ions were deposited and concentrated on AuNPs (32 nm) via Au^+-I^- interaction. The pulse laser radiation was applied to induce the enhancement of the desorption and ionization efficiency of gold–iodide hybrid cluster ions from the AuNPs surfaces. In addition, the AuNPs-MCEM allow the accurate quantification of I⁻ ions in high-salinity real samples (i.e., edible salt sample and urine) with LOD as low as 50 nM that provides a simple and rapid analysis for I⁻ ions with high sensitivity and selectivity in biological samples.
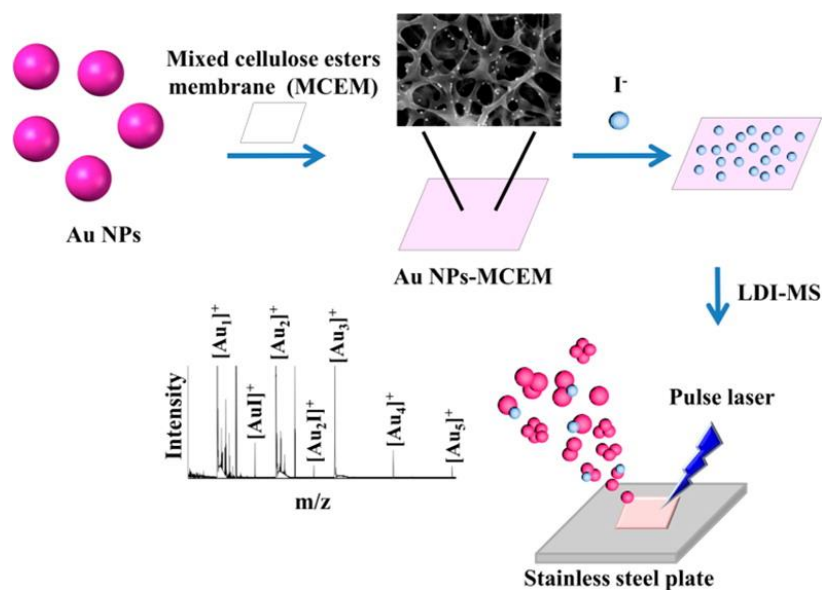
Figure 1.6 Schematic representation of the preparation of the Au NPs-MCEM substrate and its application for the determination of I⁻ Ions via LDI-MS.[27]

In 2013, Sangsuwan and coworkers[28] prepared poly(acrylic acid) (PAA) brushes on glass surface via photolithography and surface-initiated reversible addition–fragmentation chain transfer (RAFT) polymerization. The carboxyl groups of PAA brushes can act as reducing moieties for *in situ* synthesis of AuNPs to adsorb the laser energy and transfer to analyte in ionization step for MS analysis which can also function as concentrating and selective probes for thiol-containing peptide. The glass surface-modified by PAA brushes and immobilized with AuNPs (AuNPs-PAA) were used as a substrate for surface-assisted laser desorption/ionization mass spectrometry (SALDI-MS), which is capable of detecting GSH and ICNKQDCPILE peptide that has high sensitivity and selectivity with LOD as low as 0.1 and 0.05 nM, respectively.
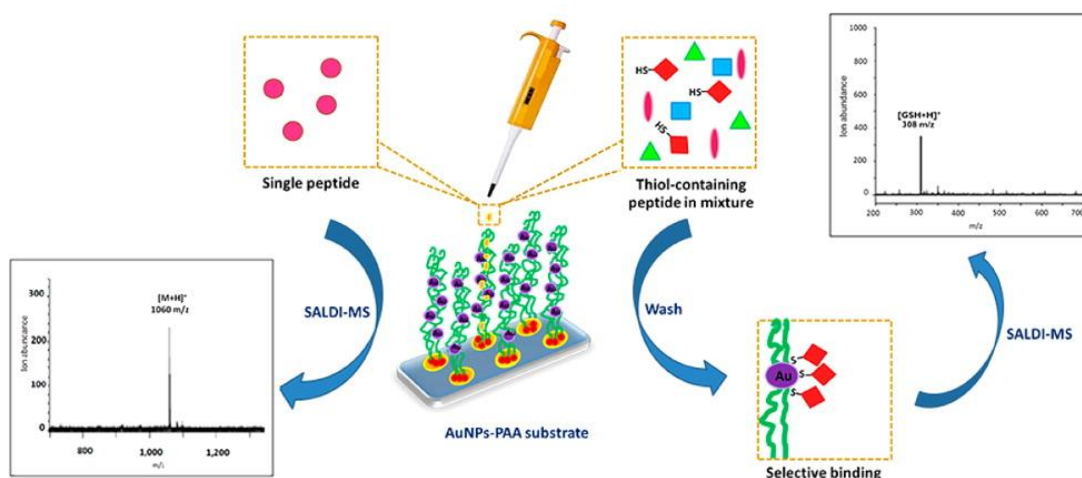
Figure 1.7 Schematic illustration of patterned PAA brushes containing AuNPs supported on a glass slide as a substrate for SALDI-MS analysis.[28]

Here in this research, the BC/CMC hydrogel was developed into a platform that can specifically accommodate thiol-containing biomarker detection via LDI-MS by incorporating *in situ* generated AuNPs into the hydrogel. It is anticipated that such approach would avoid AuNPs from aggregation and the good distribution of AuNPs within the matrix of the hydrogel should lead to effective sample ionization and detection during LDI-MS analysis. The highly swellable BC/CMC hydrogel should also allow for simultaneous sample collection from aqueous-based clinically relevant media (i.e. sweat, saliva, urine). GSH was selected as a model of thiol-containing biomarker to be analyzed as it is an important biomarker in some diseases, such as Alzheimer's, Parkinson's, cancer, aging and heart problem.

1.2 Objectives

1. To prepare and characterize the BC/CMC/AuNPs composites.
2. To study the usage of the BC/CMC/AuNPs for analyte collection and as a substrate for LDI-MS analysis.

1.3 Scope of investigation

The stepwise investigation was carried out as follows

1. Literature survey for related research work.

2. Preparation and characterization of BC/CMC hydrogel.

3. Preparation of characterization of BC/CMC/AuNPs composite

4. LDI-MS analysis of GSH on BC/CMC/AuNPs composite.

CHAPTER II

EXPERIMENTAL

2.1 Materials

Bacterial cellulose (BC) produced by *Acetobacter xylinum* was obtained from Thai-nanocellulose Co. Ltd. (Phatthalung, Thailand). Carboxymethyl cellulose (CMC), as sodium salt with a typical $\overline{M}_W$ of 250,000 g mol^{-1} and degree of substitution of 1.20, hydrogen tetrachloroaurate (HAuCl$_4$·3H$_2$O) and trisodium citrate dihydrate (C$_6$H$_5$Na$_3$O$_7$·2H$_2$O) were purchased from Sigma-Aldrich, USA. Sulfuric acid (H$_2$SO$_4$), Hydrochloric acid (HCl), nitric acid (HNO$_3$) and acetonitrile (CH$_3$CN) were commercially available from Merck, Germany. L-Glutathione in reduced form (GSH) was purchased from Tokyo Chemical Industry Co. Ltd. (Japan). Human plasma from pooled human blood in lyophilized form was purchased from Sigma-Aldrich, USA. Ultrapure distilled water (MilliQ water) was obtained after purification using a Millipore Milli-Q system (USA) that involves reverse osmosis, ion exchange, and a filtration step (18.2 MΩ cm resistance).

2.2 Characterization

2.2.1 Attenuated Total Reflectance-Fourier Transform Infrared Spectroscopy (ATR-FTIR)

The freeze-dried BC hydrogels were characterized by attenuated total reflectance-Fourier transform infrared spectroscopy (ATR-FTIR) using a Nicolet Impact 6700 FT-IR spectrometer with 32 scans at resolution 4 cm. A frequency of 500-4000 cm^{-1} was collected by using TGS detector.

2.2.2 Dynamic Light Scattering (DLS)

The particle size of AuNPs formed in solution by chemical reduction was analyzed by dynamic light scattering (DLS). The AuNPs suspension was placed in a cuvette and measured at 25 $^{\circ}$C three times for each sample using Malvern Nano ZSP Instruments Ltd., UK to determine the intensity average size distribution of AuNPs.

2.2.3 UV-Visible Spectroscopy

The swollen BC hydrogels with a dimension of 10x30 mm^2 were adhered to the inner wall of a quartz cuvette (10 mm) which was filled with MilliQ water. UV-visible absorbance of the swollen BC hydrogels having AuNPs was determined by UV-visible spectrometry (Agilent 8453 UV–vis spectrometer, USA).

2.2.4 Field Emission Scanning Electron Microscopy (FE-SEM)

The morphology of BC hydrogels dried in a critical point dryer (Leica EM CPD300, Leica Microsystems, Germany) was observed under a field emission scanning electron microscope (FE-SEM; JEOL JSM-7610F, Oxford X-Max 2, Japan). The size of fibers of BC hydrogel was calculated by averaging from 100 randomly measured fibers measured by FE-SEM using SemAFore software.

2.2.5 Transmission Electron Microscopy (TEM)

The morphology and size of AuNPs were analyzed by transmission electron microscope (TEM; Philips TECNAI 20, UK). To investigate the morphology of AuNPs by TEM, the frozen BC hydrogels having incorporated AuNPs were broken into pieces

followed by an addition of 100 µL of MilliQ water to prepare suspension. A 10 μL of the suspension was dropped three times on a carbon-coated copper grid which was then dried in a desiccator before TEM analysis. The size of observed AuNPs was calculated by averaging from 50 randomly measured particles analyzed by TEM using SemAFore software.

2.2.6 X-ray Diffraction (XRD)

The crystallinity of the freeze-dried BC hydrogels was characterized by x-ray diffractometer (XRD; SmartLab 30 kV/PC, Rigaku, Japan). with Cuka radiation operated at 40kV and 30mA. The measurements were recorded in a 2θ range of 5-80 degree with a scan rate of 2 degree/min. The percentage of crystallinity of BC was calculated using the following equation;

$$\text{Crystallinity (\%)} = \frac{\text{Area of crytalline peaks}}{\text{Area of all peak}} \times 100 \qquad \text{(eq 2.1)}$$

2.2.7 Thermogravimetric Analysis (TGA)

Thermogravimetric analysis (TGA) of the freeze-dried BC hydrogels was performed using a Pyris 1 TGA thermal analyzer (Perkin Elmer, USA). Samples were cut into pieces and filled in a Teflon pan. TGA was performed with a heating rate of 20 °C/min over a range of 50–700 °C under a flowing nitrogen atmosphere at 20.0 mL/min.

2.3 Experimental Procedure

2.3.1 Preparation of BC/CMC Hydrogel

BC sheet was cut into spherical shape (0.5 cm diameter). CMC solution ((0.5% (w/v)) was prepared by dissolving CMC (0.5 g) in MilliQ water (100 mL) at 60°C for 1 h. The cut BC hydrogel was immersed in a 24-well plate each containing 1 mL CMC solution. The 24-well plate containing BC hydrogel was shaken for 3 h at room temperature. The resulting BC/CMC hydrogel was stirred in MilliQ water for 3 days to get rid of excess CMC.

2.3.2 Preparation of BC/CMC/AuNPs Composites

Following the method reported by Kusolkamabot, *et al.*[29], the prestine BC and BC/CMC hydrogels were immersed in a round bottom flask containing HAuCl$_4$ solution (25 mL) of different concentration (0.024, 0.120, and 0.240 mM) for 30 min. The HAuCl$_4$ solution containing the hydrogels were heated to boil and 1 mL of tri-sodium citrate solution of different concentration (1, 5, 10 mg/mL) was added. The solutions were then heated to 100°C for 3 h. The resulting BC/AuNPs or BC/CMC/AuNPs composites were taken out from the solution, rinsed with MilliQ water then kept at 4°C in MilliQ water until use.

2.3.3 Measurement of Swelling Ratio

The swelling ratio of hydrogels was estimated following the Japan Industrial Standard (JIS) K8150[30]. The dried BC hydrogels were weighed (W$_d$) and immersed in MilliQ water for 1, 3 and 24 h at room temperature. The swollen hydrogels were placed on a stainless steel net of 30 meshes, blot-dried by lint-free paper (Kimtech Science Kimwipe, Kimberly-Clark, USA) and then weighed (W$_s$). The swelling ratio was calculated using the following equation:

$$\text{Swelling ratio} = (W_s - W_d)/W_d \qquad\qquad (eq\ 2.2)$$

2.3.4 Determination of AuNPs Composition

AuNPs content in the BC/AuNPs and BC/CMC/AuNPs composites were determined by Inductively coupled plasma atomic emission spectroscopy (ICP-AES). The calibration curve of gold solution was generated from Au^{3+} solution having concentration in a range of 0.1 – 15 ppm. Each piece of the freeze-dried composite was digested in a test tube containing H_2SO_4 (60 %w/v, 0.5 mL) at 60^oC for 3 h. The digested solution was added with 10 drops of aqua regia solution (1:3 (v/v) of HNO_3: HCl) before filtered through a PTFE syringe filter (0.45 μm). The volume of the filtered solution was adjusted to 10 mL with MilliQ water. The solution was then subjected to ICP-AES analysis. The composition of AuNPs is reported in %w/w with respect to the total weight of the composite.

2.3.4. LDI-MS analysis

LDI-MS analysis was performed by matrix-assisted laser desorption/ionization mass spectrometer (MALDI-TOF; Autoflex III, Bruker, U.S.A). The BC/CMC/AuNPs composite was tested as a preconcentration platform for GSH, a model of thiol-containing biomarker. The GSH standard solution of varied concentration (50, 100, 500, 1000, 2500, 5000, 10000 nM, N = 3) were prepared. Then, 200 μL of GSH standard solution was dropped on the freeze-dried composite. Afterwards, the composite was soaked in MilliQ water for 24 h to wash excess GSH remained on the surface of the composite. The composites uptaken GSH of varied concentration were subjected to LDI-MS analysis to generate a calibration curve. For real sample analysis, human plasma solution was spiked with GSH solution of varied concentration (1,350, 2,700, 5,400 nM) which is in a range of GSH level in plasma. The prepared GSH-spiked human plasma solution was subjected to protein precipitation method[31] by firstly adding acetonitrile with volume two third of the volume of the plasma solution. The mixed solution was then centrifuged at 4000 rpm for 30 min. The supernatant was

then dropped on the composite, rinsed with MilliQ water for 24 h and subjected to LDI-MS analysis. The limit of detection (LOD) was calculated from standard deviation of blank signal (SD) and the slope of calibration curve (S) using the following equation:

$$LOD = 3.3SD/S \qquad\qquad (eq\ 2.3)$$

CHAPTER III

RESULT AND DISCUSSION

3.1 Preparation of BC/CMC/AuNPs composites

The BC/CMC hydrogel was obtained by soaking the BC sheet in CMC solution (0.5% w/v). As shown in **Figure 3.1**, the BC/CMC hydrogel exhibits greater degree of swelling than the pristine BC hydrogel which confirmed the enhancement of swelling after CMC incorporation. Upon chemical reduction of $HAuCl_4$ within the matrix of both BC and BC-CMC hydrogels, *in situ* generated AuNPs were successfully incorporated as verified by the pink-to red color of the resulting BC/CMC/AuNPs composites. The color became darker as a function of $HAuCl_4$ concentration in both BC (**Figure 3.1, A1-A3**) and BC/CMC (**Figure 3.1, B1-B3**) matrices implying that there was greater quantity of AuNPs formed as the $HAuCl_4$ concentration increased. The color intensity of the BC/CMC/AuNPs composites appear lighter than that of the BC/AuNPs composites which may be explained by the better AuNPs distribution in the former which is more swelling than the latter.
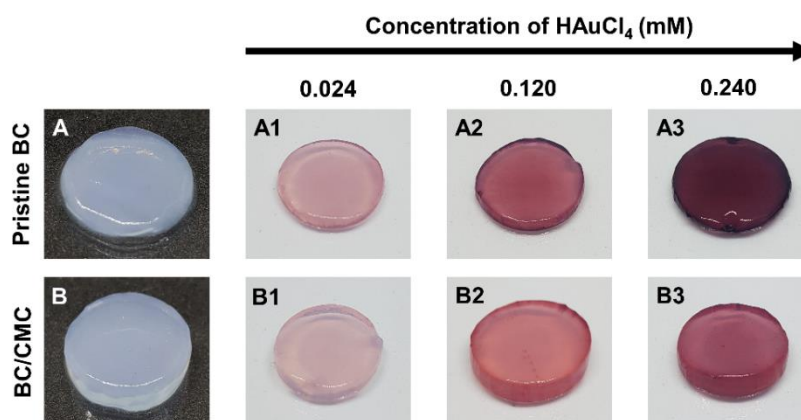

Figure 3.1 Photographs of pristine BC (A) and BC/CMC (B) before and after in situ incorporating AuNPs using $HAuCl_4$ having concentration of 0.024 mM (A1 and B1), 0.120 mM (A2 and B2) and 0.240 mM (A3 and B3), respectively.

3.2 Swelling behavior of hydrogel

The swelling ratios of all hydrogels were estimated by Japan Industrial Standard (JIS) K8150 as shown in **Figure 3.2**. Upon CMC incorporation, the swelling of the BC/CMC hydrogels increased more than 50% of the original BC hydrogel at all soaking time (1, 3, and 24 h). After 3 and 24 h of soaking, the *in situ* AuNPs introduction using the $HAuCl_4$ solution of at least 0.120 mM slightly increase the swelling of the resulting BC/AuNPs composite. The $HAuCl_4$ concentration to 0.120 mM yielded BC/CMC/AuNPs composite with good swelling property almost equivalent to that of the BC/CMC hydrogel (with non-significant difference between BC/CMC and BC/CMC/AuNPs composite at $p < 0.05$). The BC/CMC/AuNPs composite prepared at this condition was therefore used for further study.
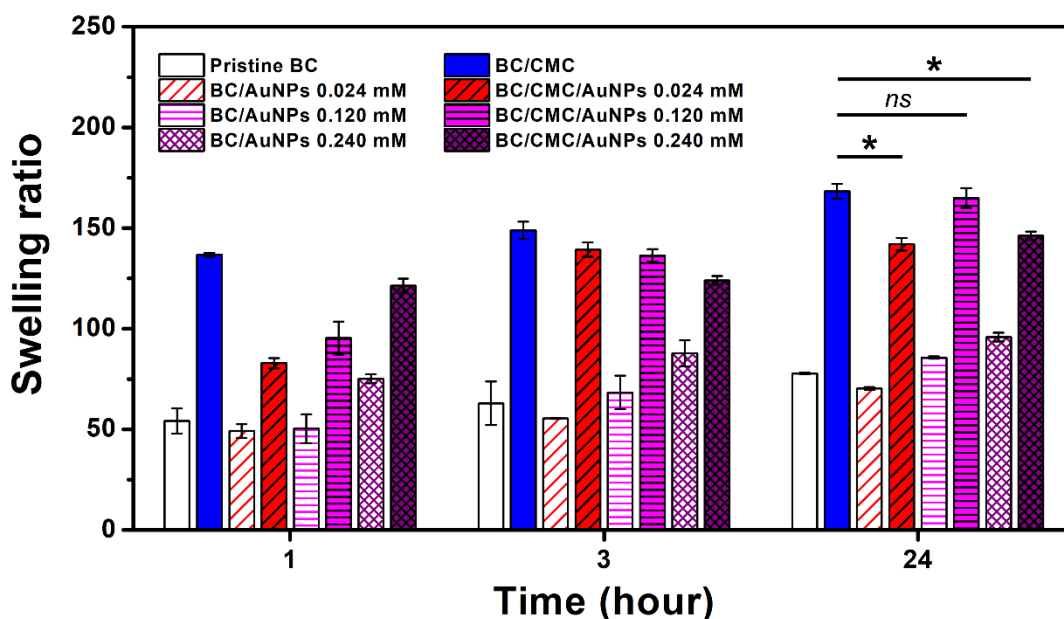

Figure 3.2 Swelling ratio of hydrogels using Japanese Industrial Standard K8150 (JIS K8150). *****: significantly different at the $p < 0.05$. *ns*: non-significantly different at the $p < 0.05$

3.3 Characterization of BC/CMC/AuNPs

Dried BC/CMC/AuNPs hydrogels were characterized by ATR-FTIR. The FT-IR spectra (**Figure 3.3**) showed the C=O stretching of carboxylate group (COO⁻) at 1590 cm^{-1} and C-H stretching of methylene group at 1415 cm^{-1} of CMC. For BC, BC/CMC and BC/CMC/AuNPs, the O-H stretching, and C-H stretching were observed at 3340 and 2890 cm^{-1}, respectively, both of which are characteristic peaks of cellulose type I.[32] Moreover, the C–O–C stretching of 1,4-β-D-glucoside linkage was observed at 1162 cm^{-1} and the C–O bending and C–O–C pyranose ring skeletal vibration were observed at 1108 and 1054 cm^{-1}, respectively. The same bands were also observed for pristine BC, BC/CMC and BC/CMC/AuNPs composite, indicating that the CMC and AuNPs incorporation did not cause changes in the chemical structure of BC.
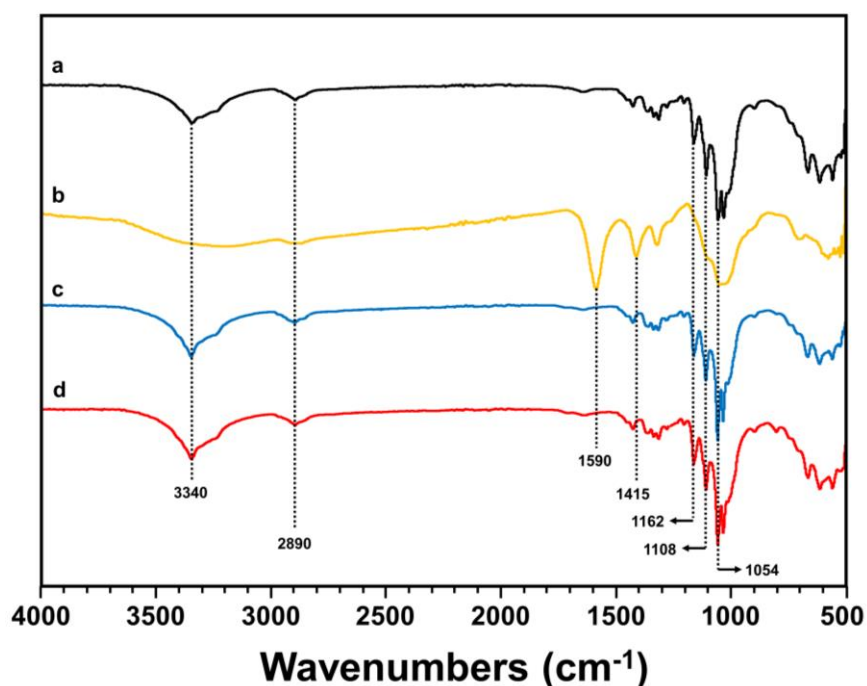

Figure 3.3 FT-IR spectra of (a) pristine BC, (b) CMC, (c) BC/CMC, and (d) BC/CMC/AuNPs prepared using 0.120 mM $HAuCl_4$.

As evaluated by DLS, the average hydrodynamic diameter of AuNPs formed concurrently in the solution was around 30 nm with narrow polydispersity index (PDI). The PDI values in a range of 0.1 – 0.4 implied that the AuNPs are uniform in size **(Table 3.1)**. The size of AuNPs are quite independent of the HAuCl$_4$ concentration. The presence of AuNPs in the BC/CMC/AuNPs composite was verified by UV-visible spectroscopy. As illustrated in **Figure 3.4A**. the characteristic peak of AuNPs in the BC/CMC/AuNPs composite was observed at 527 nm, assignable to the LSPR band of AuNPs.[33] Such peak was absent in the UV-Vis spectra of the pristine BC and BC/CMC hydrogel. The morphology of AuNPs formed within the BC/CMC/AuNPs composite was evaluated by TEM. As shown in **Figure 3.4B**, the embedded AuNPs are spherical in shape and uniform in size with diameter around 13.27 ± 2.00 nm. The AuNPs concurrently formed in the solution had diameter of around 14.27 ± 0.41 which is quite similar to the embedded AuNPs. Apparently, the size of AuNPs evaluated by TEM was much smaller than that analyzed by DLS implying that the AuNPs were highly swollen under hydrated condition. This is unlikely if the AuNPs were stabilized by citrate ions. It is hypothesized that there may be some CMC leaking out from the BC/CMC into the solution during the *in situ* AuNPs formation. Such CMC may wrap around the AuNPs concurrently formed in the solution so that the AuNPs exhibited much larger diameter than what is expected. This hypothesis needs to be proven by TEM analysis of the organic-stained AuNPs.

Table 3.1 Particle size and PDI of AuNPs formed in solution using varied concentration of $HAuCl_4$ during the preparation of BC/AuNPs and BC/CMC/AuNPs as evaluated by DLS.

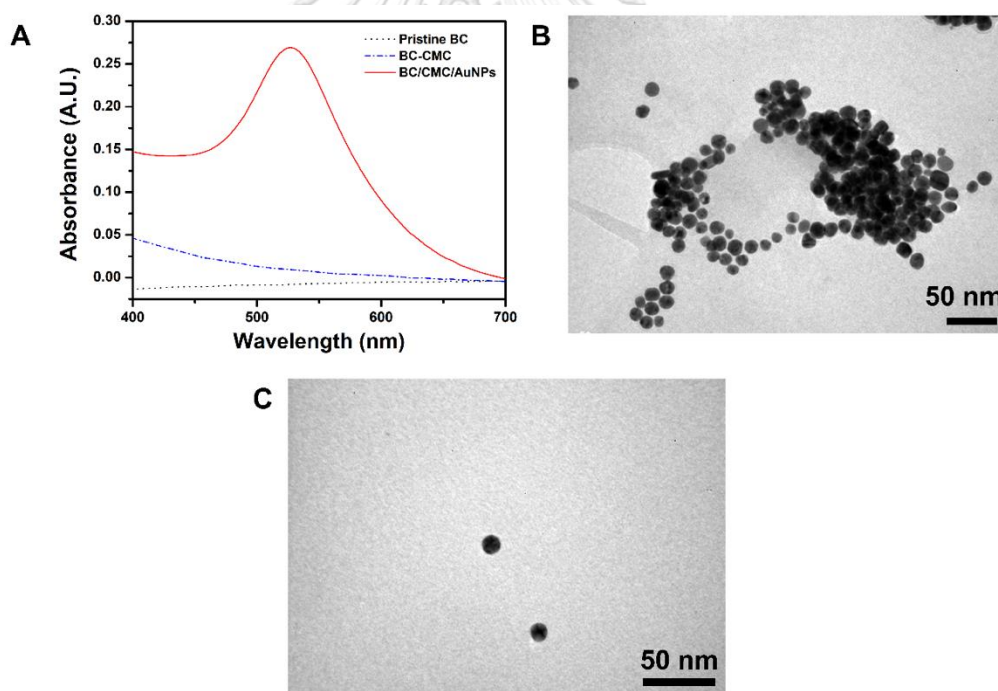| Hydrogels	$HAuCl_4$ (mM)	Particle size (nM)	PDI
BC/AuNPs	0.024	31.94 ± 1.47	0.289
	0.120	29.51 ± 0.59	0.128
	0.240	29.46 ± 0.49	0.260
BC/CMC/AuNPs	0.024	31.56 ± 1.88	0.233
	0.120	30.37 ± 0.46	0.217
	0.240	31.54 ± 0.80	0.388

Figure 3.4 UV-visible spectra of BC, BC/CMC hydrogel and BC/CMC/AuNPs composite (A), TEM micrograph of embedded AuNPs in the BC/CMC/AuNPs (B) and formed AuNPs in solution (C).

Morphological structures of the BC, BC/CMC and BC/CMC/AuNPs were evaluated by FE-SEM. **Figure 3.5A-C** showed fibrous network of BC with diameter of the fibers of around 25 ± 2.4 nm. The BC fibers of the BC/CMC and BC/CMC/AuNPs (**Figure 3.5B-C**) seemed to be more loosely packed than those within the pristine BC (**Figure 3.5A**). However, the packing of BC fibers became slightly denser after the AuNPs incorporation (**Figure 3.5C**). **Figure 3.5a-b** show the physical appearance of hydrogels. The thickness of pristine BC hydrogel (**Figure 3.5a**) was around 3 mm and increased to 4.5 mm after CMC incorporation (**Figure 3.5b**) but decreased to 3.5 mm after AuNPs fabrication (**Figure 3.5c**). This thickness variation agrees quite well with the fiber packing.
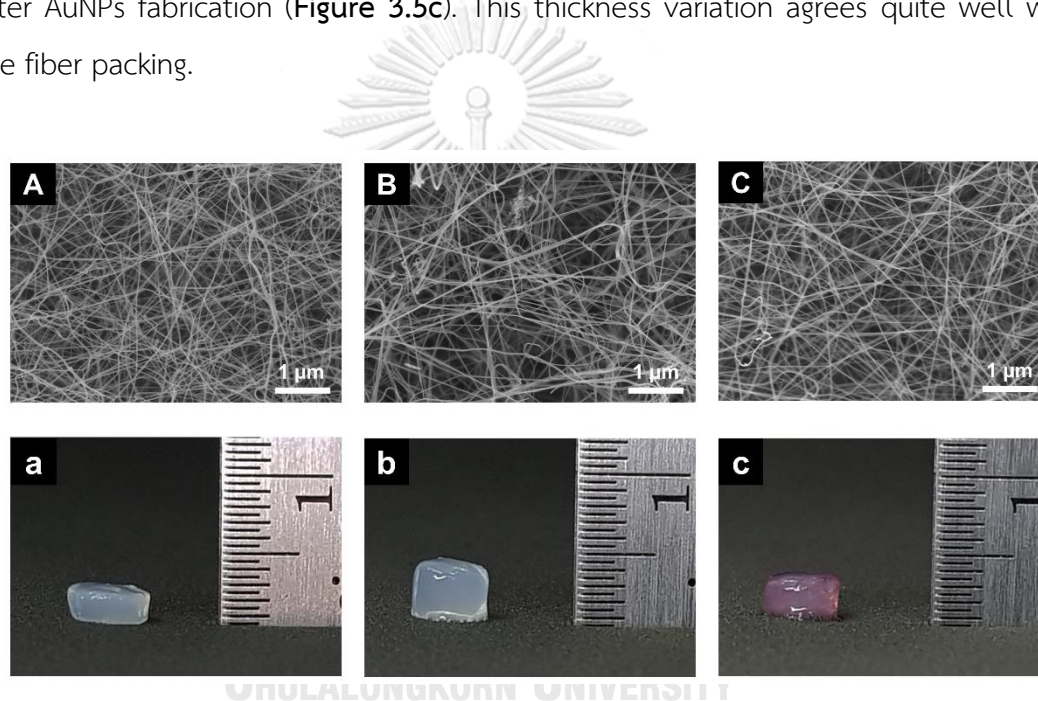

Figure 3.5 FE-SEM micrographs and photographs of pristine BC (A, a), BC-CMC (B, b) and BC-CMC-AuNPs (C, c).

To confirm the crystal structure of BC and AuNPs, XRD analysis was performed. XRD pattern of CMC powder displayed a broad peak at 20.7° corresponding to the amorphous nature of the pure CMC. The dried BC displayed three diffraction peaks with 2θ at 14.5°, 16.8° and 22.6° corresponding to the (110), (110), and (200) planes of cellulose I[34], respectively (**Figure 3.6A**). The degrees of crystallinity of BC/CMC and BC/CMC/AuNPs were found to be only slightly lower than

the pristine BC, suggesting that the high crystallinity of BC was maintained despite the incorporation of CMC and AuNPs (**Table 3.2**). The fact that the XRD patterns as well as their corresponding peak intensity of all hydrogels did not significantly change implied that the crystal structure of BC remained unaltered after CMC incorporation and *in situ* chemical reduction to generate AuNPs. XRD pattern of the BC/CMC/AuNPs in **Figure 3.6B** exhibited a peak at $38.5°$ which can be assigned to the (111) crystal planes of gold.[35] verifying the presence of AuNPs formed within the composite.
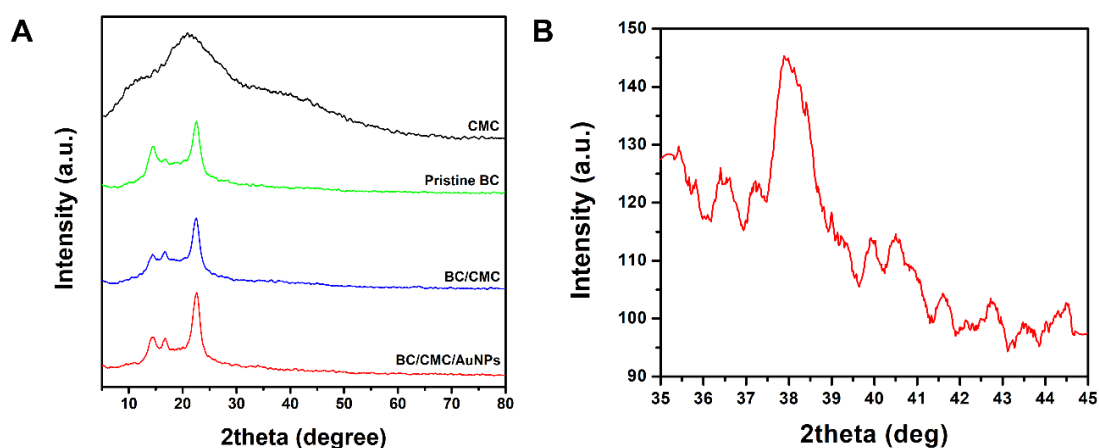
Figure 3.6 XRD patterns of CMC, BC, BC/CMC, BC/CMC-AuNPs (A) and magnified XRD pattern of BC-CMC-AuNPs in the 2θ region of $35-45°$ (B).

Table 3.2 Crystallinity of BC, BC/CMC and BC/CMC/AuNPs hydrogels

Sample	%Crystallinity
Pristine BC	72.41
BC/CMC	71.02
BC-CMC-AuNPs	71.59

TGA and derivatized thermogravimetric (DTG) curves are demonstrated in **Figure 3.7A and B**, respectively. The pristine BC exhibited a weight loss of 93% in a temperature range of $250 – 400°C$ which was the degradation of the main cellulose

skeleton. The degradation profile of BC/CMC appears in a similar range with 90% weight loss suggesting that the degradation is dominated by the BC. The BC/CMC/AuNPs composite exhibited a weight loss of 95% in a higher temperature range of 275 – 430 ^{o}C suggesting the presence of AuNPs in BC/CMC matrix improves the thermal stability of hydrogels. The BC, BC/CMC and BC/CMC/AuNPs were completely decomposed at 501, 535 and 730 ^{o}C, respectively.
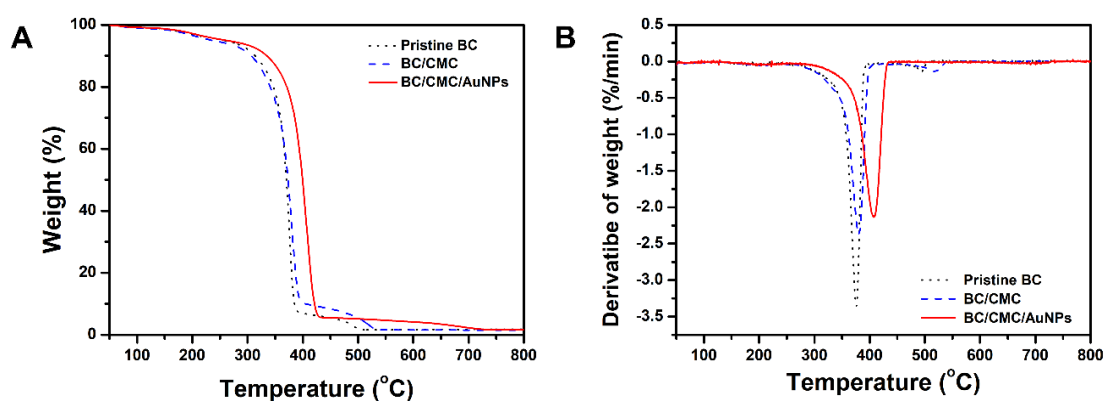

Figure 3.7 TGA curves (A) and DTG curves (B) of BC, BC/CMC, and BC/CMC/AuNPs hydrogels.

3.4 Determination of AuNPs Composition

To quantitate the gold content in the BC/AuNPs and BC/CMC/AuNPs composites, all samples were digested in the H_2SO_4 to transform fiber into sugar and prevent the trapped gold ion inside the BC matrix followed by an addition of aqua regia to digest AuNPs into Au^{3+} ions. The samples were determined by ICP-AES by using Au^{3+} standard solution of varied concentrations (0.1 – 15 ppm, N=3) to generate a calibration curve as shown in **Figure 3.8.** According to ICP-AES analysis, the gold content of BC/AuNPs composite increased proportionally as a function of $HAuCl_3$ concentration as shown in **Table 3.3** By employing the same $HAuCl_4$ concentration, the quantity of gold nanoparticles in the BC/CMC/AuNPs composite was approximately half of that in the BC/AuNPs composite. This may presumably be

explained as a result of lower local concentration of Au^{3+} within the more swollen BC/CMC/AuNPs composite than that within the BC/AuNPs composite. The BC/CMC/AuNPs composite that was further used for LDI-MS analysis was prepared using $HAuCl_4$ concentration of 0.120 mM. This substrate contains 1.24 ± 0.22 %w/w.
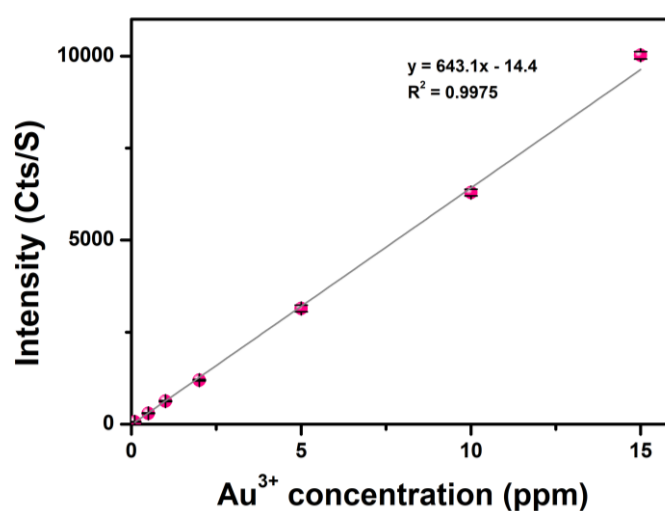
Figure 3.8 Calibration curve of Au^{3+} standard solution for determination of AuNPs by ICP-AES.

Table 3.3 Gold content in the BC/AuNPs and BC/CMC/AuNPs composites prepared using varied $HAuCl_4$ concentration

$HAuCl_4$ concentration (mM)	AuNPs content (%w/w)	
	BC/AuNPs	BC/CMC/AuNPs
0.024	0.52 ± 0.08	0.27 ± 0.35
0.120	2.10 ± 0.17	1.24 ± 0.22
0.240	4.10 ± 0.50	1.93 ± 0.26

3.5 LDI-MS analysis

The BC-CMC-AuNPs composite was tested for GSH absorption, a model of thiol-containing biomarker by being immersed in GSH standard solutions of varied concentrations (50 – 10,000 nM, N = 3). From the mass spectrum of GSH 500 nM (**Figure 3.9**), there are three dominant peaks of [GSH+H]+ (m/z 307.9), [GSH+Na]+ (m/z 307.9) and [GSH+K]+ (m/z 307.9). The calibration curve showing a linear relationship between ion abundance and GSH concentration (Figure 3.10) strongly suggested that the developed BC/CMC/AuNPs composite can potentially be used as a sample collection platform for quantitative analysis of GSH. A high sensitivity of GSH detection with a low limit of detection (LOD) of 54.1 nM which was calculated using eq 2.3. and a wide linear detection range of 50 – 10,000 nM can be reached with a good linear correlation (R^2 = 0.9961). This also covers GSH level in human plasma [19]. To evaluate the feasibility of the method for the analysis of real samples, the composite was applied to the determination of GSH in human plasma with varied concentration. GSH was spiked into human plasma samples. Recoveries of the spiked amount of GSH in the diluted human plasma samples were obtained in a range of 91.36 – 103.98% (**Table 3.4**) These results indicated the good reliability of the method for GSH analysis in complicated biological samples.

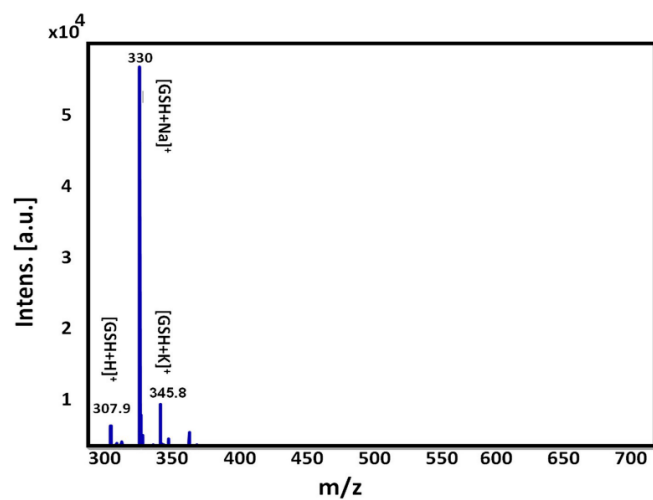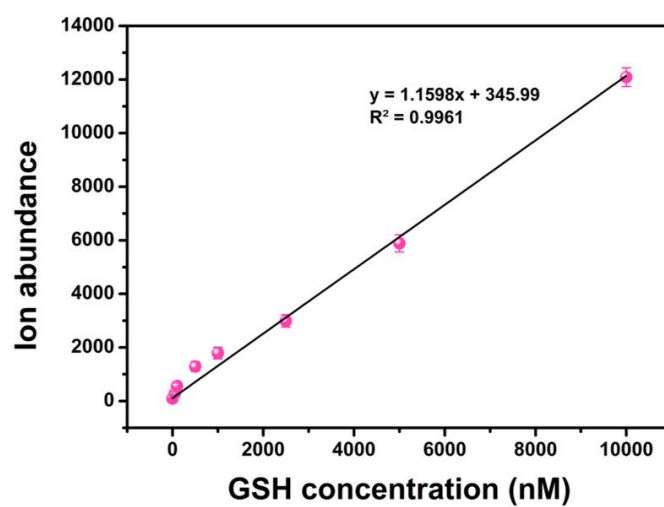**Figure 3.9** Mass spectra of GSH 500 nM by using optimized BC/CMC/AuNPs as substrate.

Figure 3.10 Calibration curve of GSH standard solution as analyzed by LDI-MS using BC/CMC/AuNPs composite as the preconcentration/sample collection platform.

Table 3.4 Recovery percentage of GSH spiked in diluted human plasma with varied GSH concentration.

Spiked GSH concentration (nM)	Recovery (%)
1350	103.98
2700	91.36
5400	101.69

The comparison of analytical performance between this platform together with the LDI-MS analysis and other methods is presented in **Table 3.1**. In general, GSH determination in human plasma requires highly sensitive and selective methods of which LODs are in a range of nM. For the GSH analysis by colorimetry using AuNPs and 2,2′–azino–bis(3–ethylbenzothiazoline–6–sulfonic acid) (ABTS) oxidized by Ag^+ ion [37, 40] exhibited a linear range of 500 - 1,250 nM and 500 - 4,000 nM with LODs of 500 and 59 nM, respectively. The fluorescence analysis using dual-mode carbon quantum dots (CQDs) and AuNPs[31] also exhibited a lower LOD of 50 nM with a linear range of 100 - 600 nM. For the method having higher sensitivity, High-Performance Liquid Chromatography (HPLC) coupled with electrochemical detection [39] gave a wider linear range of 500 - 10,000 nM with LOD as low as 200 nM. Moreover, spectrofluorimetric method using graphene as adsorbent for solid-phase extraction and N-(4,4-difluoro-5,7-dimethyl-4-bora-3a,4a-diaza-s-indacene-3-yl)methyl)iodoacetamide (BODIPY Fl-C1-IA) as a fluorescent probe [36] to derivatize GSH yielded a low LOD of 0.01 nM with a linear range of 0.05 - 200 nM. Unlike the methods mentioned above, the LDI-MS analysis employing the developed BC/CMC/AuNPs composite as a platform for sample collection not only can be used for quantitative analysis of GSH with a favorably wider linear range and the low LOD, but the analysis can also be done without the requirement for extra steps of extraction and/or preconcentration prior to analysis.

Table 3.5 Analytical characteristics of different methods used for GSH analysis in human plasma.

Ref.	Methods	Materials or sensing elements	Linear range (nM)	LOD (nM)
[36]	Spectrofluorimetry	BODIPY Fl-C$_1$-IA Solid-phase extraction using graphene as adsorbent	0.05 – 200	0.01
[37]	Colorimetry	AuNPs	500 – 1,250	500
[38]	Electrochemistry	Nickel hexacyanoferrate film/CTAB/AuNPs Pt electrode	200 – 1,000	80
[31]	Fluorescence	CQDs and AuNPs	100 – 600	50
[39]	HPLC-Electrochemistry	Screen-Printed Gold Electrodes	500 – 10,000	200
[40]	Colorimetry	Ag$^+$ ion and (ABTS	100 – 4,000	59
This work	LDI-MS	BC/CMC/AuNPs	50 – 10,000	54.1

CHAPTER IV
CONCLUSION AND SUGGESTIONS

In summary, we have successfully developed BC/CMC/AuNPs composites by incorporating CMC and AuNPs via simple soaking the pristine BC in CMC solution and HAuCl$_4$ solutions, respectively and followed by heating to induce *in situ* chemical reduction. The amount of *in situ* generated AuNPs can be varied as a function of the HAuCl$_4$ concentration from ICP-AES analysis. The swelling of BC/CMC/AuNPs hydrogels increased more than 50% of the original BC hydrogel. The BC/CMC/AuNPs were characterized by FT-IR, UV-visible spectroscopy, FE-SEM, TEM, XRD and TGA. The crystallinity and fibrous nature of the original BC was not significantly affected by the CMC and AuNPs incorporation with fiber size around 25 nm. TGA and DTG data suggested that the presence of AuNPs in in BC/CMC matrix improved the thermal stability of hydrogel with higher decomposition temperature. The embedded AuNPs are uniform size with diameter around 13 nm in BC matrix which also confirmed from crystal plane of gold by XRD analysis and the characteristic absorption band of AuNPs in UV-vis spectra. The BC/CMC/AuNPs composite prepared using 0.120 mM HAuCl$_4$ was found to be the appropriate condition for GSH biomarker absorption because of its good swelling property. The composite was tested to generate a calibration curve by using LDI-MS. The quantitative analysis of GSH which is a biomarker for Alzheimer's diagnostics via LDI-MS exhibited high sensitivity and low LOD of 54.1 nM and the linear range of 50 – 10,000 nM which covers GSH level in human plasma. Moreover, this platform could be used for GSH analysis in spiked human plasma which good recoveries. Our on-going investigation is to determine pre-concentration efficiency.

According to all result mentioned above, all experiments indicated that the developed BC/CMC/AuNPs composites could be prepared by simple protocol with low cost of materials. Moreover, the composites had a potential to be a sample collection platform for quantitative analysis of biomarker and applied for medical diagnostics in the future.
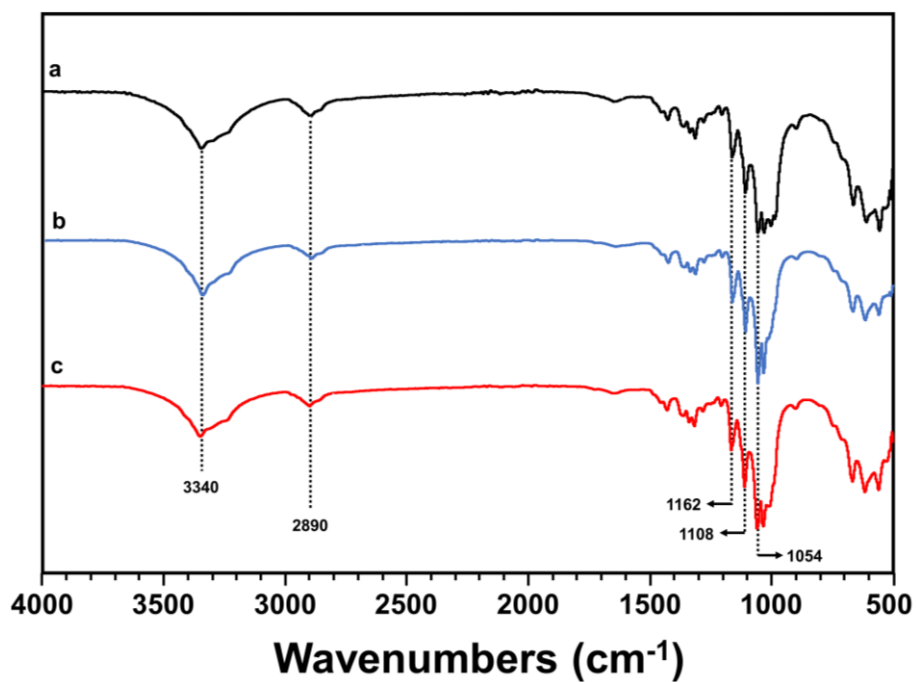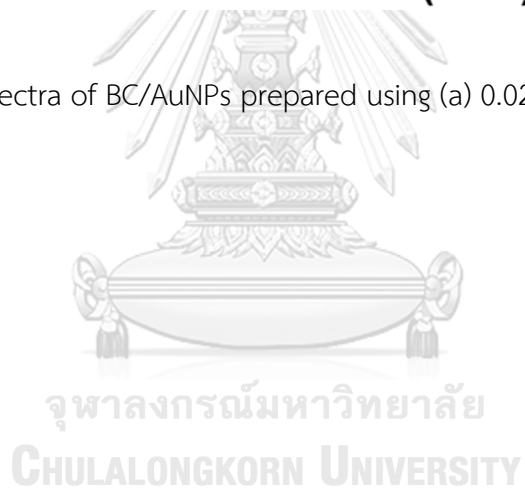
APPENDIX

Figure A1 FT-IR spectra of BC/AuNPs prepared using (a) 0.024 mM, (b) 0.120 mM and 0.240 mM HAuCl$_4$.
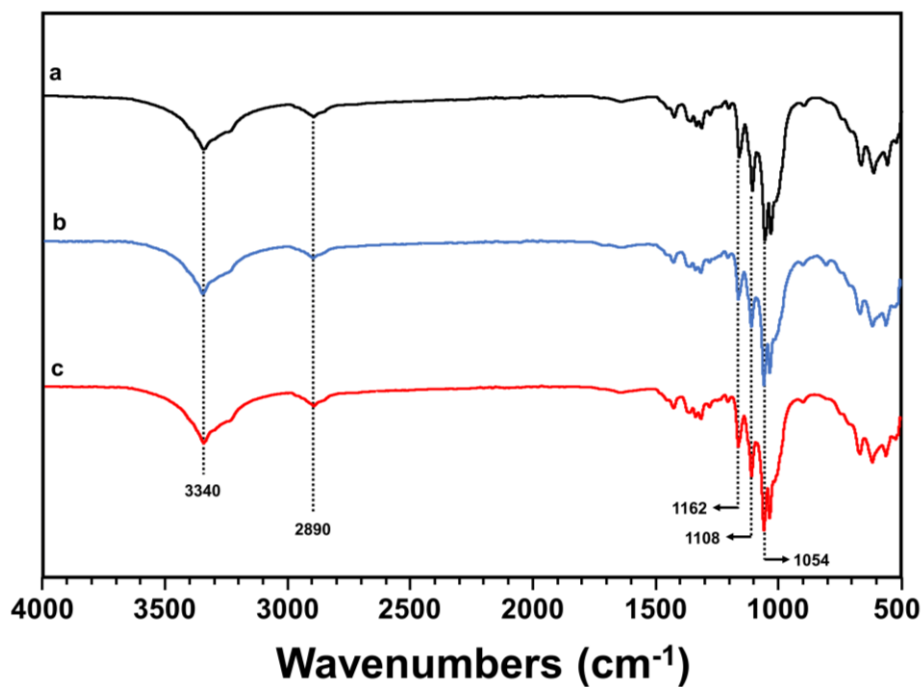
Figure A2 FT-IR spectra of BC/CMC/AuNPs prepared using (a) 0.024 mM, (b) 0.120 mM and 0.240 mM HAuCl$_4$.
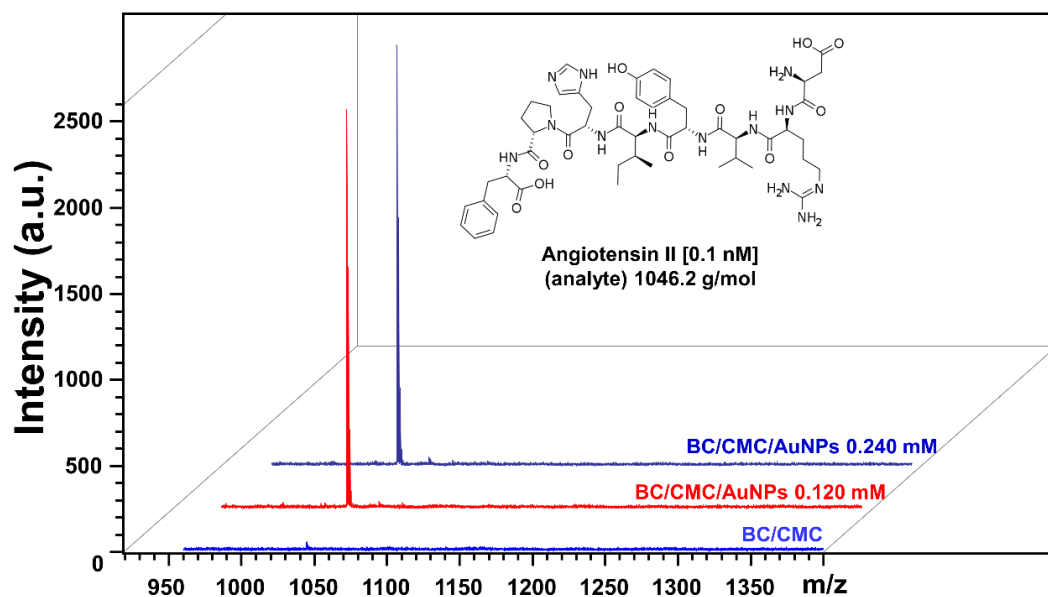

Figure A3 Mass spectra of angiotensin II (0.1 nM) by using BC/CMC and BC/CMC/AuNPs as substrate.
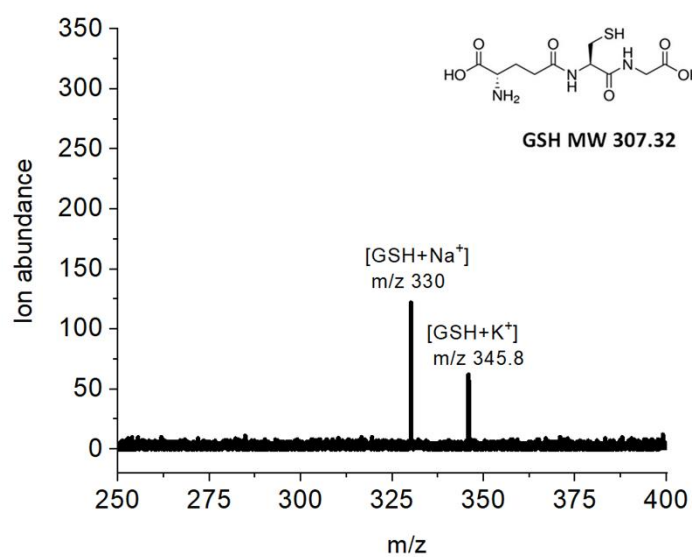
Figure A4 Mass spectrum of GSH standard solution (50 nM) by using optimized BC/CMC/AuNPs as substrate.

Figure A5 Mass spectra of 10x diluted human plasma by using optimized BC/CMC/AuNPs as substrate.

Figure A6 Mass spectrum of GSH spiked in 10x diluted human plasma (1250 nM) by using optimized BC/CMC/AuNPs as substrate.

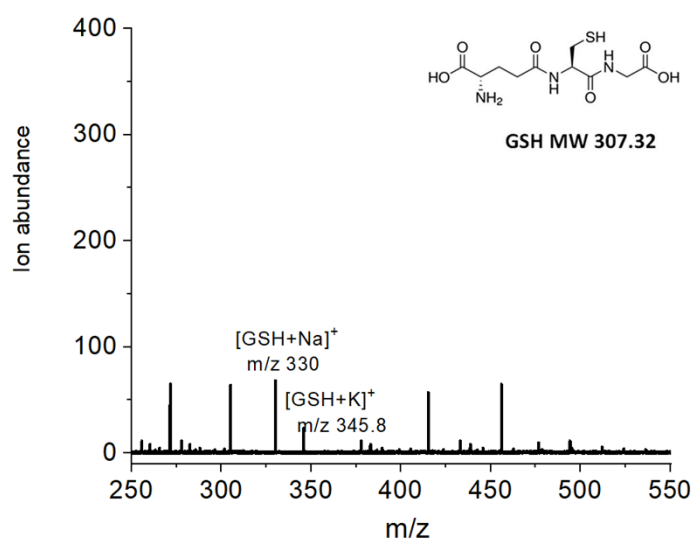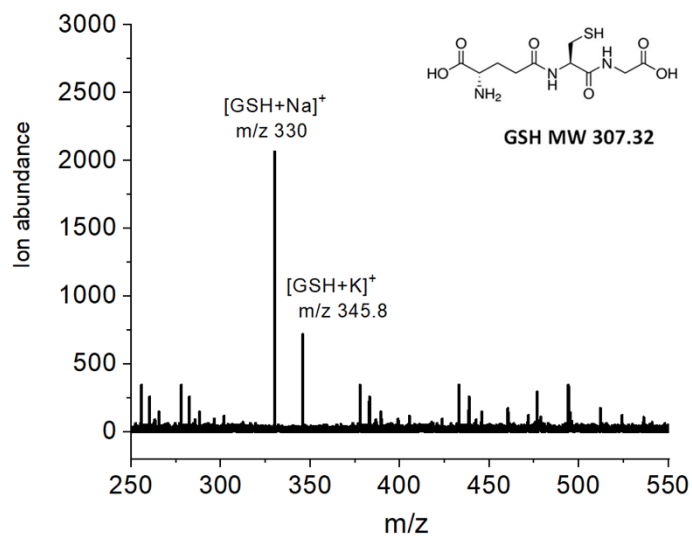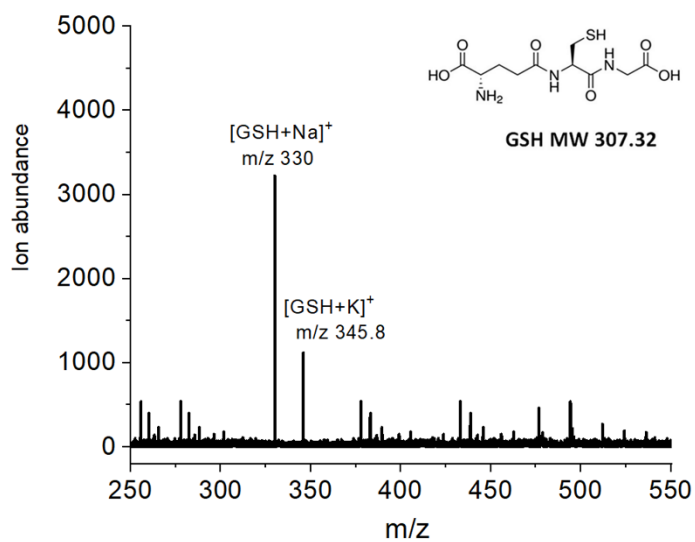**Figure A7** Mass spectrum of GSH spiked in 10x diluted human plasma (2700 nM) by using optimized BC/CMC/AuNPs as substrate.
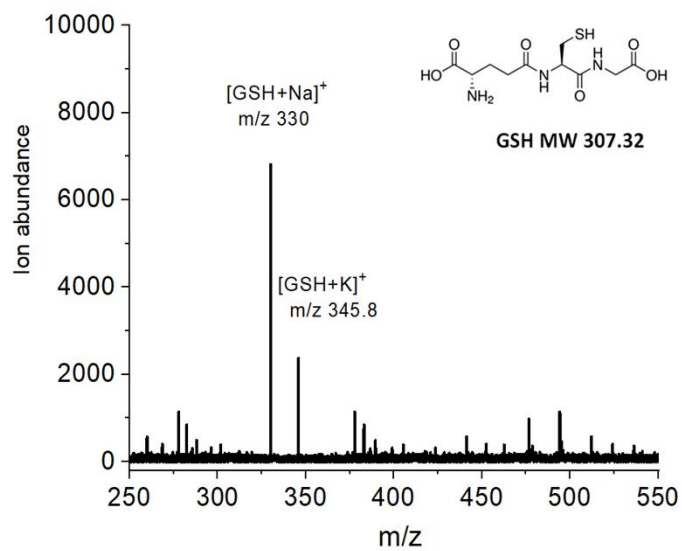
Figure A8 Mass spectrum of GSH spiked in 10x diluted human plasma (5400 nM) by using optimized BC/CMC/AuNPs as substrate.

REFERENCES

1. Gorgieva, S.; Trček, J., Bacterial Cellulose: Production, Modification and Perspectives in Biomedical Applications. *Nanomaterials (Basel)* **2019,** *9* (10), 1352.

2. Azeredo, H. M. C.; Barud, H.; Farinas, C. S.; Vasconcellos, V. M.; Claro, A. M., Bacterial Cellulose as a Raw Material for Food and Food Packaging Applications. **2019,** *3* (7).

3. Chan, C.; Shin, J.; Jiang, S., Development of Tailor-Shaped Bacterial Cellulose Textile Cultivation Techniques for Zero-Waste Design. *Clothing and Textiles Research Journal* **2017,** *36*, 0887302X1773717.

4. Jin, M.; Chen, W.; Li, Z.; Zhang, Y.; Zhang, M.; Chen, S., Patterned bacterial cellulose wound dressing for hypertrophic scar inhibition behavior. *Cellulose* **2018,** *25*.

5. Lin, S.-B.; Hsu, C.-P.; Chen, L.-C.; Chen, H.-H., Adding enzymatically modified gelatin to enhance the rehydration abilities and mechanical properties of bacterial cellulose. *Food Hydrocolloids* **2009,** *23* (8), 2195-2203.

6. Chen, H.-H.; Chen, L.-C.; Huang, H.-C.; Lin, S.-B., In situ modification of bacterial cellulose nanostructure by adding CMC during the growth of Gluconacetobacter xylinus. *Cellulose* **2011,** *18* (6), 1573-1583.

7. Torres, F. G.; Arroyo, J. J.; Troncoso, O. P., Bacterial cellulose nanocomposites: An all-nano type of material. *Materials Science and Engineering: C* **2019,** *98*, 1277-1293.

8. Yang, G.; Xie, J.; Deng, Y.; Bian, Y.; Hong, F., Hydrothermal synthesis of bacterial cellulose/AgNPs composite: A "green" route for antibacterial application. *Carbohydrate Polymers* **2012,** *87* (4), 2482-2487.

9. Pal, S.; Nisi, R.; Stoppa, M.; Licciulli, A., Silver-Functionalized Bacterial Cellulose as Antibacterial Membrane for Wound-Healing Applications. *ACS Omega* **2017,** *2* (7), 3632-3639.

10. Chen, M.; Kang, H.; Gong, Y.; Guo, J.; Zhang, H.; Liu, R., Bacterial Cellulose

Supported Gold Nanoparticles with Excellent Catalytic Properties. *ACS Applied Materials & Interfaces* **2015,** *7* (39), 21717-21726.

11.   Wei, H.; Rodriguez, K.; Renneckar, S.; Leng, W.; Vikesland, P. J., Preparation and evaluation of nanocellulose–gold nanoparticle nanocomposites for SERS applications. *Analyst* **2015,** *140* (16), 5640-5649.

12.   de Lima Fontes, M.; Meneguin, A. B.; Tercjak, A.; Gutierrez, J.; Cury, B. S. F.; dos Santos, A. M.; Ribeiro, S. J. L.; Barud, H. S., Effect of in situ modification of bacterial cellulose with carboxymethylcellulose on its nano/microstructure and methotrexate release properties. *Carbohydrate Polymers* **2018,** *179*, 126-134.

13.   Siripongpreda, T.; Somchob, B.; Rodthongkum, N.; Hoven, V. P., Bacterial cellulose-based re-swellable hydrogel: Facile preparation and its potential application as colorimetric sensor of sweat pH and glucose. *Carbohydrate Polymers* **2021,** *256*, 117506.

14.   Li, G.; Sun, K.; Li, D.; Lv, P.; Wang, Q.; Huang, F.; Wei, Q., Biosensor based on bacterial cellulose-Au nanoparticles electrode modified with laccase for hydroquinone detection. *Colloids and Surfaces A: Physicochemical and Engineering Aspects* **2016,** *509*, 408-414.

15.   Morales-Narváez, E.; Golmohammadi, H.; Naghdi, T.; Yousefi, H.; Kostiv, U.; Horák, D.; Pourreza, N.; Merkoçi, A., Nanopaper as an Optical Sensing Platform. *ACS Nano* **2015,** *9* (7), 7296-7305.

16.   Mayeux, R., Biomarkers: potential uses and limitations. *NeuroRx* **2004,** *1* (2), 182-188.

17.   Mandal, P. K.; Saharan, S.; Tripathi, M.; Murari, G., Brain Glutathione Levels – A Novel Biomarker for Mild Cognitive Impairment and Alzheimer's Disease. *Biological Psychiatry* **2015,** *78* (10), 702-710.

18.   Wu, G.; Fang, Y.-Z.; Yang, S.; Lupton, J. R.; Turner, N. D., Glutathione Metabolism and Its Implications for Health. *The Journal of Nutrition* **2004,** *134* (3), 489-492.

19.   Rani, P.; Krishnan, S.; Rani Cathrine, C., Study on Analysis of Peripheral Biomarkers for Alzheimer's Disease Diagnosis. *Front Neurol* **2017,** *8*, 328-328.

20.   Simoska, O.; Duay, J.; Stevenson, K. J., Electrochemical Detection of

Multianalyte Biomarkers in Wound Healing Efficacy. *ACS Sensors* **2020,** *5* (11), 3547-3557.

21. Zheng, Z.; Geng, W.-C.; Gao, J.; Wang, Y.-Y.; Sun, H.; Guo, D.-S., Ultrasensitive and specific fluorescence detection of a cancer biomarker via nanomolar binding to a guanidinium-modified calixarene. *Chem Sci* **2018,** *9* (8), 2087-2091.

22. Yang, P.-W.; Hsu, I. J.; Chang, C.-W.; Wang, Y.-C.; Hsieh, C.-Y.; Shih, K.-H.; Wong, L.-F.; Shih, N.-Y.; Hsieh, M.-S.; Hou, M. T.-K.; Lee, J.-M., Visible-absorption spectroscopy as a biomarker to predict treatment response and prognosis of surgically resected esophageal cancer. *Scientific Reports* **2016,** *6* (1), 33414.

23. Chiu, N.-F.; Yang, H.-T., High-Sensitivity Detection of the Lung Cancer Biomarker CYFRA21-1 in Serum Samples Using a Carboxyl-MoS2 Functional Film for SPR-Based Immunosensors. **2020,** *8* (234).

24. Crutchfield, C. A.; Thomas, S. N.; Sokoll, L. J.; Chan, D. W., Advances in mass spectrometry-based clinical biomarker discovery. *Clin Proteomics* **2016,** *13*, 1-1.

25. Chu, H.-W.; Unnikrishnan, B.; Anand, A.; Mao, J.-Y.; Huang, C.-C., Nanoparticle-based laser desorption/ionization mass spectrometric analysis of drugs and metabolites. *Journal of Food and Drug Analysis* **2018,** *26* (4), 1215-1228.

26. Chiang, C.-K.; Chiang, N.-C.; Lin, Z.-H.; Lan, G.-Y.; Lin, Y.-W.; Chang, H.-T., Nanomaterial-Based Surface-Assisted Laser Desorption/Ionization Mass Spectrometry of Peptides and Proteins. *Journal of the American Society for Mass Spectrometry* **2010,** *21* (7), 1204-1207.

27. Li, Y.-J.; Tseng, Y.-T.; Unnikrishnan, B.; Huang, C.-C., Gold-Nanoparticles-Modified Cellulose Membrane Coupled with Laser Desorption/Ionization Mass Spectrometry for Detection of Iodide in Urine. *ACS Applied Materials & Interfaces* **2013,** *5* (18), 9161-9166.

28. Sangsuwan, A.; Narupai, B.; Sae-ung, P.; Rodtamai, S.; Rodthongkum, N.; Hoven, V. P., Patterned Poly(acrylic acid) Brushes Containing Gold Nanoparticles for Peptide Detection by Surface-Assisted Laser Desorption/Ionization Mass Spectrometry. *Analytical Chemistry* **2015,** *87* (21), 10738-10746.

29. Kusolkamabot, K.; Sae-ung, P.; Niamnont, N.; Wongravee, K.; Sukwattanasinitt, M.; Hoven, V. P., Poly(N-isopropylacrylamide)-Stabilized Gold Nanoparticles in

Combination with Tricationic Branched Phenylene-Ethynylene Fluorophore for Protein Identification. *Langmuir* **2013,** *29* (39), 12317-12327.

30. Sultana, S.; Islam, M.; Dafader, N.; Haque, M. E. u.; Nagasawa, N.; Tamada, M., Effect of mono- and divalent salts on the properties of carboxymethyl cellulose hydrogel under irradiation technique. *International Journal of Chemical Sciences* **2012,** *10*.

31. Shi, Y.; Pan, Y.; Zhang, H.; Zhang, Z.; Li, M.-J.; Yi, C.; Yang, M., A dual-mode nanosensor based on carbon quantum dots and gold nanoparticles for discriminative detection of glutathione in human plasma. *Biosensors and Bioelectronics* **2014,** *56,* 39-45.

32. Wang, S.-S.; Han, Y.-H.; Ye, Y.-X.; Shi, X.-X.; Xiang, P.; Chen, D.-L.; Li, M., Physicochemical characterization of high-quality bacterial cellulose produced by Komagataeibacter sp. strain W1 and identification of the associated genes in bacterial cellulose production. *RSC Advances* **2017,** *7* (71), 45145-45155.

33. Zhou, X.; Zhao, Z.; He, Y.; Ye, Y.; Zhou, J.; Zhang, J.; Ouyang, Q.; Tang, B.; Wang, X., Photoinduced synthesis of gold nanoparticle–bacterial cellulose nanocomposite and its application for in-situ detection of trace concentration of dyes in textile and paper. *Cellulose* **2018,** *25* (7), 3941-3953.

34. Zhijiang, C.; Guang, Y., Bacterial cellulose/collagen composite: Characterization and first evaluation of cytocompatibility. **2011,** *120* (5), 2938-2944.

35. Chen, Y.; Chen, S.; Wang, B.; Yao, J.; Wang, H., TEMPO-oxidized bacterial cellulose nanofibers-supported gold nanoparticles with superior catalytic properties. *Carbohydrate Polymers* **2017,** *160*, 34-42.

36. Huang, K.-J.; Jing, Q.-S.; Wei, C.-Y.; Wu, Y.-Y., Spectrofluorimetric determination of glutathione in human plasma by solid-phase extraction using graphene as adsorbent. *Spectrochimica Acta Part A: Molecular and Biomolecular Spectroscopy* **2011,** *79* (5), 1860-1865.

37. Hu, B.; Cao, X.; Zhang, P., Selective colorimetric detection of glutathione based on quasi-stable gold nanoparticles assembly. *New Journal of Chemistry* **2013,** *37* (12), 3853-3856.

38. He, H.; Du, J.; Hu, Y.; Ru, J.; Lu, X., Detection of glutathione based on nickel

hexacyanoferrate film modified Pt ultramicroelectrode by introducing cetyltrimethylammonium bromide and Au nanoparticles. *Talanta* **2013,** *115,* 381-385.

39. Cavanillas, S.; Serrano, N.; Díaz-Cruz, J. M.; Ariño, C.; Esteban, M., Commercial Screen-Printed Gold Electrodes for the Detection and Quantification of Aminothiols in Human Plasma by Liquid Chromatography with Electrochemical Detection. *Electroanalysis* **2014,** *26* (3), 581-587.

40. Li, Y.; Liu, X.; Zhang, R., Sensitive and selective colorimetric detection of glutathione in human plasma with 2,2′–azino–bis(3–ethylbenzothiazoline–6–sulfonic acid) and Ag+ ion. *Spectrochimica Acta Part A: Molecular and Biomolecular Spectroscopy* **2017,** *173,* 880-885.

VITA

NAME	Panlop Lormaneenopparat
DATE OF BIRTH	12 April 1995
PLACE OF BIRTH	Bangkok
INSTITUTIONS ATTENDED	Bachelor Degree of Science in Applied Chemistry from Faculty of Science and Engineering, Kasetsart University Chalermphrakiat Sakon Nakhon Province Campus, Sakon Nakhon in 2017
HOME ADDRESS	326/24 Naiklongbangplakod, Phrasamutchedee, Samutprakan 10290
PUBLICATION	Proceeding: February 2020, Oral presentation in IUMRS-ICA 2020 at Faculty of Science, Chiang Mai University, Chiang Mai, Thailand

จุฬาลงกรณ์มหาวิทยาลัย
CHULALONGKORN UNIVERSITY